

Civil Engineering Journal

(E-ISSN: 2476-3055; ISSN: 2676-6957)

Vol. 11, No. 10, October, 2025



Methodology for Seismic Vulnerability Assessment of Pre-Code Masonry Buildings Using Region-Specific Data

Kristina Milkova 1*0, Elena Dumova-Jovanoska 10

¹ Faculty of Civil Engineering, Ss. Cyril and Methodius University in Skopje, Skopje, North Macedonia.

Received 24 July 2025; Revised 15 September 2025; Accepted 22 September 2025; Published 01 October 2025

Abstract

This study presents a comprehensive methodology for evaluating the seismic vulnerability of existing pre-code masonry structures through a multidisciplinary approach that integrates region-specific building typologies with site-specific seismic input. A key gap motivating this work is the absence of fragility curves for masonry structures typical of the region despite their prevalence and high seismic exposure. Recognizing the importance of reliable Seismic Hazard Assessment (SHA) in risk evaluation, a scenario-based Neo-Deterministic Seismic Hazard Assessment (NDSHA) approach was employed. This method incorporates a detailed understanding of the region's tectonic regime, active fault systems, earth crust structure, and historical seismicity to produce realistic site-specific response spectra for analysis. The seismic capacity of the structures was assessed using multiple iterations of a nonlinear static (pushover) analysis, accounting for uncertainties in the material and geometric input parameters. The structural displacement was used as the primary damage index, and the damage was classified into five discrete damage grades. Consequently, new fragility and reliability curves were developed: (i) a general set for unreinforced masonry (URM) structures, (ii) four regional sets corresponding to distinct zones within the country, and (iii) two sets differentiating between regular and irregular plan configurations. The novelty of this study lies in the development of region-specific fragility curves for URM buildings, providing urgently needed tools for seismic risk assessment and supporting mitigation strategies and decision-making at the local and national levels.

Keywords: Masonry; Vulnerability Assessment; Neo-Deterministic Hazard Assessment; Fragility Curves, Reliability Curves.

1. Introduction

Earthquakes are a formidable challenge in civil engineering. Their unpredictable and uncontrollable nature continues to pose serious problems, prompting key questions: How can we fully protect structures from such hazardous forces, and how can we ensure that existing structures are adequately prepared? Structural vulnerability represents the quantifiable weaknesses of structures exposed to earthquakes of varying intensity [1, 2]. When combined with seismic hazard assessments, this information provides essential insights into structural resilience and enables the prediction of potential damage from future earthquakes [3, 4]. Recent seismic events in North Macedonia, Albania, and Croatia have heightened public concern and emphasized the ongoing need for the seismic design of new structures as well as risk assessment of existing structures. For example, the most recent significant earthquake in North Macedonia occurred on September 10, 2016, with a magnitude of 5.2 at a depth of 10 km, 2 km northeast of Skopje [5, 6].

The aging building stock, combined with new load demands from evolving building requirements, compels engineers to develop advanced methodologies for the assessment of existing structures [7]. Uncertainties in seismic hazard characterization and input definitions make seismic vulnerability assessments inherently comprehensive and

^{*} Corresponding author: milkova@gf.ukim.edu.mk





© 2025 by the authors. Licensee C.E.J, Tehran, Iran. This article is an open access article distributed under the terms and conditions of the Creative Commons Attribution (CC-BY) license (http://creativecommons.org/licenses/by/4.0/).

multidisciplinary [8]. Modern seismic codes place equal emphasis on evaluating existing structures as they do on designing new ones [9, 10]. To complement these codes, guidelines and action plans have been established to support post-earthquake interventions, including repair and strengthening measures [11, 12]. However, the lack of institutional preparedness often becomes evident after earthquakes, particularly when the observed damage exceeds expectations, despite shaking levels remaining within the design parameters [13, 14].

A key tool for addressing these challenges is the use of fragility curves and damage probability matrices, which link seismic hazards at a specific site with the expected structural impacts [15]. Vulnerability, defined as the likelihood that a structure will experience a given level of damage under certain ground motions, is a useful indicator for identifying structures requiring strengthening. Existing methodologies incorporate uncertain parameters such as load, material properties, and building design, which lead to a wide range of outcomes [16]. These approaches, which are applicable to diverse structural systems, vary from simple observational methods to advanced computational models that capture the full structural complexity [17, 18]. Calvi et al. [18] provided a detailed overview of the evolution of vulnerability assessment methods, whereas Kassem et al. [19] summarized widely used empirical and analytical approaches. Methodologies are generally categorized into four groups: empirical, judgmental, analytical, and hybrid. The key advantage of the analytical approach to vulnerability assessment is its independence from post-earthquake damage data, although the calibration of the models against observed damage is always advisable. In North Macedonia, post-earthquake damage observations are relatively limited, despite the region's moderate to high seismicity, and the application of modern analytical procedures represents an appropriate and efficient method for estimating structural vulnerability and assessing potential earthquake losses.

Fragility curves are central to seismic loss estimation and planning [20-22]. When integrated with structural databases classified by location, material, and typology, they provide a strong foundation for the development of comprehensive seismic risk maps [23]. Several international methodologies, including HAZUS, EMS-98, and Risk-UE, have proposed fragility curves for various structural classes. These frameworks are often used to develop procedures for seismic risk mitigation on a territorial scale [24]. However, these approaches rely on broad classifications and fail to capture the diversity of the construction typologies found in practice. Critical aspects such as local material properties, workmanship, traditional techniques, and region-specific design practices are frequently oversimplified, despite their significant influence on seismic response. Therefore, developing fragility curves tailored to local construction practices and informed by empirical earthquake performance is essential for improving risk assessment and mitigation strategies.

Research on seismic vulnerability in the Balkans has paralleled global developments. In North Macedonia, Nocevski proposed a methodology for the empirical and analytical vulnerability assessment of structural capacity curves by introducing a local damage criterion with five defined damage levels [25, 26]. Dumova–Jovanoska developed an analytical framework linking earthquake intensity to damage, expressed through vulnerability curves and damage probability matrices, and validated the approach for reinforced concrete structures in the Skopje region using synthetic earthquake records and nonlinear analysis [27]. The RISC-UE project [28] extended this line of work with methodologies for RC buildings using nonlinear time-history analyses and historical earthquake inputs. More recently, damaging earthquakes in the region, such as those in Zagreb and Petrinja, have reinvigorated efforts to develop vulnerability functions, particularly through empirical approaches supported by post-earthquake damage data [29–32]. School buildings, for example, have been the focus of recent studies that introduced novel seismic risk assessment frameworks [33, 34]. Despite this progress, fragility curves remain scarce for many building types, particularly precode unreinforced masonry (URM) structures, which are predominant in the region [35, 36]. These structures often control the extent of earthquake damage and loss. Moreover, the shared historical construction practices of ex-Yugoslav countries suggest that fragility curves developed in one nation may be applicable regionally.

In this context, the present study focuses on generating fragility curves for precode masonry structures in North Macedonia, providing a framework that can be extended across the Balkan region. This methodology integrates local building configurations, regional seismic hazard data, and structural damage modeling to produce curves that reflect the vulnerability of these structures under various earthquake scenarios. This paper presents the stepwise implementation of the proposed approach and finally develops region-specific fragility curves, considering both plan-level and regional-scale sensitivity. These results offer crucial insights for engineers, urban planners, and policymakers, enabling targeted mitigation strategies, prioritization of retrofitting interventions, and improved risk management for pre-code masonry buildings across the region.

2. Methodology Steps

In this study, a novel analytical methodology was proposed for the development of seismic fragility curves tailored to existing buildings. This methodology integrates three key input domains: (a) parameters related to the structural characteristics of buildings, (b) region-specific seismicity and geotechnical conditions, and (c) predefined damage scenarios, as illustrated in Figure 1. The proposed approach establishes a systematic framework that links region-specific building typologies, such as construction materials, structural systems, and design practices, with region-specific seismic inputs, including ground motion records and local hazard parameters. This integration facilitates the generation of fragility functions that are not only structure-specific but also contextually grounded in local seismic environments. The outcome was the development of a database of regional fragility functions for locally defined prototype structures. This

database represents a foundational step toward advancing seismic risk assessment and mitigation planning. The application of this methodology enables more accurate vulnerability estimation for the built environment, thereby providing essential input for seismic risk scenarios and prioritization of intervention measures. Furthermore, the availability of locally calibrated fragility functions can support decision makers and local authorities in formulating effective strategies and action plans for seismic risk reduction, including the allocation of resources for retrofitting and the implementation of building regulations for improved seismic resilience.

Input 1	Input 3				
Region hazard catalog	Damage catalog				
Interlinked Methodology					
Output					
Regionally defined Fragility & Reliability curves					

Figure 1. General concept

The first set of input parameters in the proposed methodology is related to the regional seismic hazard data, which are essential for establishing a realistic and context-sensitive representation of the seismic environment. Specifically, these parameters should reflect the most reliable seismic hazard model for the Republic of North Macedonia. This forms the foundation for accurately modelling the seismic inputs used in nonlinear analyses. The accurate characterization of seismic hazards is particularly critical in regions such as the Balkans, where moderate to strong earthquakes have historically caused widespread damage, and where complex tectonic settings contribute to significant spatial variability in ground motion characteristics.

The second group of inputs pertained to the structural characteristics of the building stock in the selected region. This includes parameters such as building typologies, height, age, material properties, construction quality, and presence or absence of seismic detailing. These data are essential for the development of representative computational models capable of capturing the nonlinear behavior of typical structures under seismic loading. The models should reflect the inelastic response of the structures and incorporate degradation mechanisms, such as stiffness and strength deterioration, to provide realistic predictions of damage potential. Given the wide prevalence of older, pre-code buildings across the Balkans, including masonry and poorly detailed reinforced concrete structures, these models must be calibrated using local construction practices and observed damage patterns from past earthquakes.

The third input domain is concerned with the definition of damage states or damage grades, which serve as the basis for developing the fragility curves. These damage states are typically categorized using standardized frameworks, such as the European Macroseismic Scale (EMS-98) [37] or HAZUS methodology [38], and range from slight, moderate, and extensive damage to complete collapse. Each damage state corresponds to a particular level of structural and non-structural degradation and is associated with thresholds of engineering demand parameters, such as interstory drift, plastic hinge rotation, or displacement capacity. The choice of the damage model is critical, as it governs the transition probabilities between performance states and ultimately shapes the fragility functions [39].

2.1. Definition of Seismic Hazard

Seismic hazard analysis is commonly performed using two fundamental methodologies: deterministic and probabilistic [40, 41]. Regardless of the selected approach, the assessment process typically involves modeling seismic sources, analyzing source seismicity, forecasting earthquake recurrence, and estimating ground motion attenuation. The literature extensively discusses the advantages and limitations of both deterministic and probabilistic techniques for evaluating earthquake hazards and their associated risks [42]. The choice of method should primarily consider the purpose of the hazard assessment, its intended applications, and the availability and reliability of the regional seismic data.

Probabilistic seismic hazard analysis (PSHA) [43, 44] relies on earthquake catalogs and instrumental recordings and incorporates uncertainties by estimating the probability of ground motion exceeding a given design level. In North Macedonia, seismic design codes are based on the maximum expected ground motion intensities corresponding to return periods of 50, 100, 200, 500, 1000, and 10,000 years, with a 63% probability of exceedance. Similarly, the Eurocode specifies seismic design parameters in terms of peak ground acceleration (PGA) and associated probabilities of exceedance, satisfying two primary requirements: structural collapse prevention and damage limitation. For the latter, the design ground motion was defined with a 10% probability of exceedance over reference periods of 10 and 50 years [45]. Modern seismic codes follow a performance-based design framework, typically defining acceptable damage levels as operational limits (OL), Immediate Occupancy (IO), Life Safety (LS), and Collapse Prevention (CP) [46]. The corresponding earthquake intensity for each performance level was expressed as a function of the exceedance probability over a specified period. Although the advantages and disadvantages of PSHA are well documented [47-49], key

limitations include potentially oversimplified physical assumptions, incomplete or unreliable datasets, and unrealistic intensity estimates when very low probabilities are considered.

In contrast, deterministic seismic hazard analysis (DSHA) [50, 51] evaluates hazards based on a fixed ground motion scenario defined by a specific earthquake magnitude and location. This approach yields results that are highly sensitive to assumptions regarding the scenario event and may change significantly with new data. The DSHA estimates strong-motion parameters for the maximum credible earthquake, typically assumed to occur at the nearest possible distance from the site, without considering the probability of occurrence within a given timeframe [52]. Therefore, the DSHA is often regarded as the most suitable method for defining the seismic input at the Collapse Prevention limit state. Nevertheless, its limitations include strong dependence on available data, inability to generate time-history ground motions, and exclusion of rupture directivity effects [53, 54].

In this study, a scenario-based NDSHA was employed, integrating knowledge of the region's tectonic regime, active fault characteristics, crustal structure, and historical seismicity. This multi-scenario methodology, which does not rely on ground-motion prediction equations, uses advanced physical modeling to produce the required ground-motion dataset [55, 56]. Both the response spectra and the peak values of the ground displacement, velocity, and acceleration can be derived as envelopes from a large number of potential earthquakes at the location. NDSHA has been successfully applied worldwide, including in seismic microzoning studies of urban areas, strategic structures, lifeline systems, and cultural heritage sites [57].

In North Macedonia, several major geotectonic units with distinct development and composition can be identified, each corresponding to a characteristic layered model. The zoning most commonly applied was that proposed by Arsovski [58]. To define the properties of the source—site paths, the territory was subdivided into a series of polygons reflecting lithospheric characteristics at the regional scale. For this purpose, data were integrated from multiple references, including the TRANSMED ATLAS: The Mediterranean Region from Crust to Mantle – Transect III project [59], which illustrates Mediterranean geology across nine transects through its main tectonic domains. Each polygon was then linked to a representative structural model, expressed as a stack of flat anelastic layers describing average conditions to depths of approximately 1000 km. For each of these layers, parameters such as the thickness, density, P- and S-wave velocities, and attenuation factors were specified [60, 61].

Although great unpredictability of earthquake occurrence in time and magnitude is always present, some general patterns of this phenomenon exist in three large zones, named belts: the circum-Pacific seismic belt, the Alpide earthquake belt, and the Atlantic Ringe [62]. The movement of the edges of the large tectonic plates of the lithosphere produces energy release, leading to earthquakes. Historically, the most destructive earthquakes are located along these seismic belts. North Macedonia, situated within the Alpide seismic belt, is classified as an area of moderate to high seismicity. Historical records have documented several episodes of intense seismic activity across different parts of the country. Based on the spatial distribution of events recorded in the historical earthquake catalogue, combined with seismotectonic analysis, ten distinct seismogenic regions were delineated: Skopje, Vitina, Valandovo, Mrežičko, Tetovo, Debar, Ohrid, Prespa, Bitola, and Kresna. For seismic input definition, the catalogue data were discretized into cells of $0.2^{\circ} \times 0.2^{\circ}$, with each cell characterized by the maximum magnitude observed within its boundaries, in accordance with the requirements of the NDSHA methodology. Although the use of high-tex seismic instruments in the last century has driven the knowledge of the physical process behind the earthquake significantly forward, the actual release of the earthquake energy along a fault plane is still not completely understood and complex. However, idealization has been utilized for better representation of the processes that occur before, during, and after a seismic event. In this direction, the categorization of faults by their slip direction (strike-slip and dip slip) has been applied: strike-slip, normal-slip, and reverse slip (thrust) faults [63]. The maximum value of the magnitudes reported in the earthquake catalogue is applied at every node of the cells in the defined grid. In this manner, a double-information point is created, connected with information about the properties of the seizmogenic zones on one side and for the focal mechanism on the other side. Within the NDSHA framework, a smoothing procedure was implemented to account for uncertainties associated with epicentral positioning, fault geometry, and spatial distribution of possible future earthquakes in active regions [64].

The seismic input at a specific site is assessed in the form of a response spectrum derived using the Maximum Credible Seismic Input (MCSI) methodology [65, 66], which is embedded within the Neo-Deterministic Seismic Hazard Assessment (NDSHA) framework. This advanced approach enables the estimation of upper-bound ground motion, representing the most severe level of seismic excitation that could reasonably be expected to occur at this location. This level of input is critical because it defines the seismic demand to be considered in the design of new structures or the retrofitting of existing structures, especially those of vital importance or with high exposure to risk.

The MCSI methodology was specifically applied to four selected locations of particular engineering and societal interests within the territory of the Republic of North Macedonia. The calculations were performed assuming a 5% damping ratio for the response spectra in accordance with standard engineering practices.

Six distinct families of rupture scenarios are considered to capture the full range of possible seismic excitations. These include combinations of rupture style and directivity angle as follows: bilateral rupture with 0° directivity, bilateral rupture with 180° directivity, unilateral rupture with 90° directivity, and unilateral rupture with 180° directivity.

Finally, the spectra from all the scenarios were systematically merged and enveloped to produce a comprehensive and robust estimate of the seismic input at each site. This final response spectrum serves as an upper-bound input that can be confidently used in engineering applications to ensure a high level of seismic safety and resilience. When combining the results of seismic input simulations, two components are typically considered: Max and Res, both of which represent the amplitude of the computed response spectra, as illustrated in Figure 2. The maximum plot refers to the maximum horizontal component, determined by selecting the largest spectral amplitude from the two orthogonal horizontal directions for each realization. The Res plot, on the other hand, represents the resultant horizontal component, obtained by vectorially combining the two horizontal components at each period. Consequently, Res provides a more conservative estimate of the seismic hazard because it captures the total ground motion energy more comprehensively. Each colored curve corresponds to the median response spectrum obtained from 50 stochastic realizations of the rupture process for a single scenario. These individual scenarios form the envelope of the MCSI estimate.

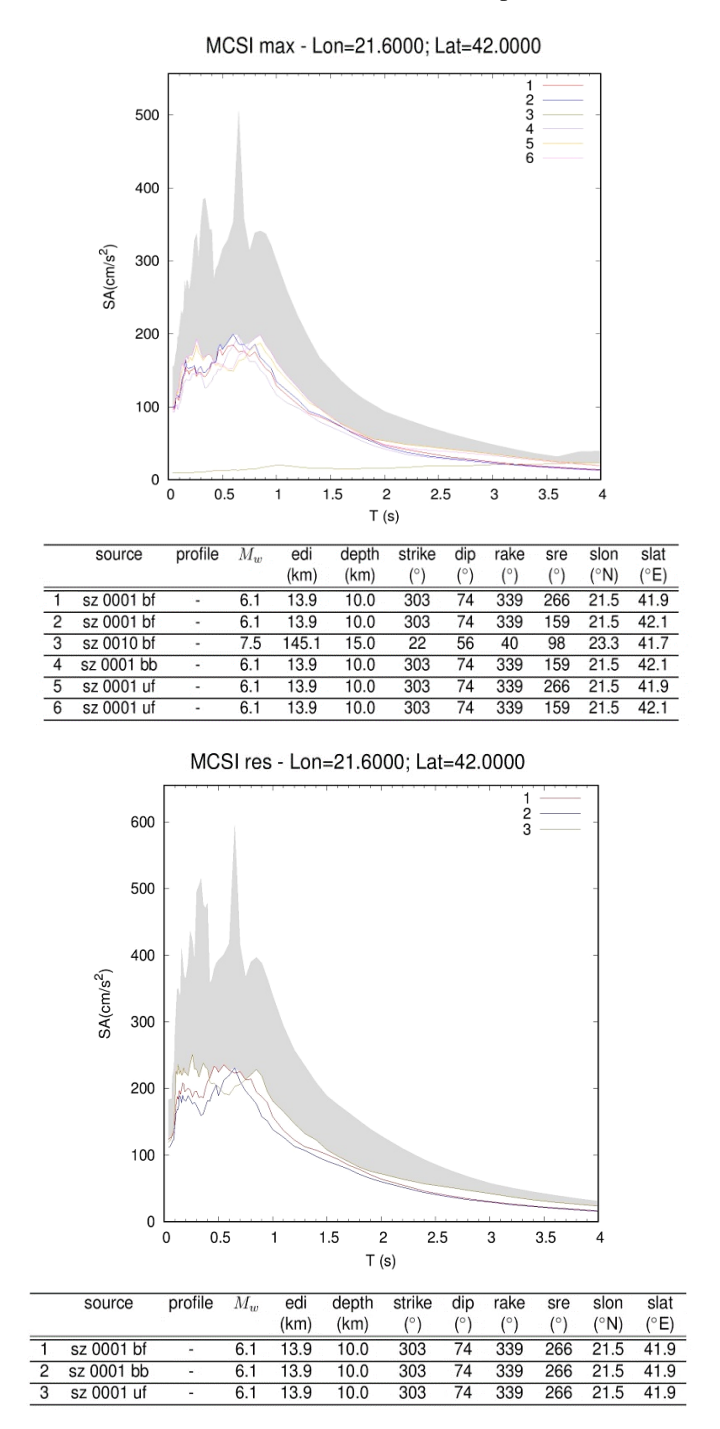


Figure 2. MCSI computed at a representative site. The top and bottom panels show the maximum and resultant horizontal components, respectively. In the source labels, bf denotes bilateral rupture with forward directivity, bb bilateral rupture with backward directivity, and uf unilateral rupture with forward directivity. At this site, no portion of the MCSI spectrum corresponds to scenarios with neutral directivity (bn or un) or unilateral rupture with backward directivity (ub).

Six scenarios are presented for the MCSI Max representation. These corresponded to three different seismic sources, each located at distinct azimuths and/or distances relative to the site under consideration. These positional differences are characterized by the source-to-receiver azimuth (sre) and epicentral distance (edi) parameters. In contrast, the MCSI Res plot includes contributions from only one seismic source but explores three different directivity configurations of the rupture process (e.g., varying orientations of rupture propagation relative to the site). This targeted approach helps assess the variability of the response due to rupture directivity effects alone.

The shaded regions in each plot indicate the variability range of the response spectra, specifically the interval between the median and the 95th percentile of the spectral acceleration distribution at each vibration period. This provides a visual quantification of the epistemic uncertainty associated with rupture modeling. Notably, the distant event, one of the three sources considered, had a significant influence on the MCSI Max spectrum only at longer vibration periods, specifically for periods greater than 3.5 seconds. This indicates the period-dependent nature of source contributions, with closer events dominating short-period responses and distant but larger-magnitude events influencing long-period behavior.

2.2. Definition of Mechanical Model of Selected Structures

The second input in the methodology presented in Figure 1 relates to the computational modeling of the selected structures. Within the framework of the SEISMOWALL project [67, 68], a total of twelve existing unreinforced masonry buildings located across different regions of the Republic of North Macedonia were selected for a detailed analysis. Each building was chosen to serve as representative of a broader typological class of similar constructions commonly found in the country. This selection was carried out as part of Work Package 1 (WP1) of the SEISMOWALL project, and it followed a set of clearly defined criteria: the primary construction material must be unreinforced masonry, the buildings must be used as public institutions, they must have been constructed prior to the 1963 Skopje earthquake, unhindered access and permission for on-site investigations must be granted by local authorities, and the buildings should be geographically distributed across various locations in the Republic of North Macedonia.

The survey and preliminary research related to the selection process revealed that buildings from this period were typically constructed using brick masonry, often combined with stone foundations or basement levels, and bonded with lime mortar, cement-lime mortar, or cement mortar, depending on local practices and material availability at the time. During this period, most residential and public buildings were constructed as unreinforced masonry structures. However, a smaller number of buildings employ confined masonry techniques, as noted in the literature [69]. Following the Skopje 1963 earthquake, a major shift occurred in construction practices across the region. The use of reinforced concrete has become standard owing to its superior performance under seismic loading. Nonetheless, a significant portion of the existing building stock, particularly outside Skopje, still consists of masonry structures.

Although some privately owned residential buildings have undergone partial reconstruction or strengthening over the years, most of the public buildings included in this study have never been assessed for seismic vulnerability or compliance with modern seismic standards. The 12 buildings analyzed within SEISMOWALL included a diverse range of public-use structures: four schools, one kindergarten, two museums, one court building, one railway station, and three administrative office buildings.

These structures were located across six cities in North Macedonia, as shown in Figure 3. For classification purposes, the buildings were grouped based on plan regularity and were divided into two typological categories: regular structures, exhibiting symmetrical and uniform plan geometry, and irregular structures, characterized by asymmetries or discontinuities in their plan layout. This typological differentiation plays an essential role in assessing the seismic behavior of masonry buildings and informs the modeling assumptions used in computational simulations.

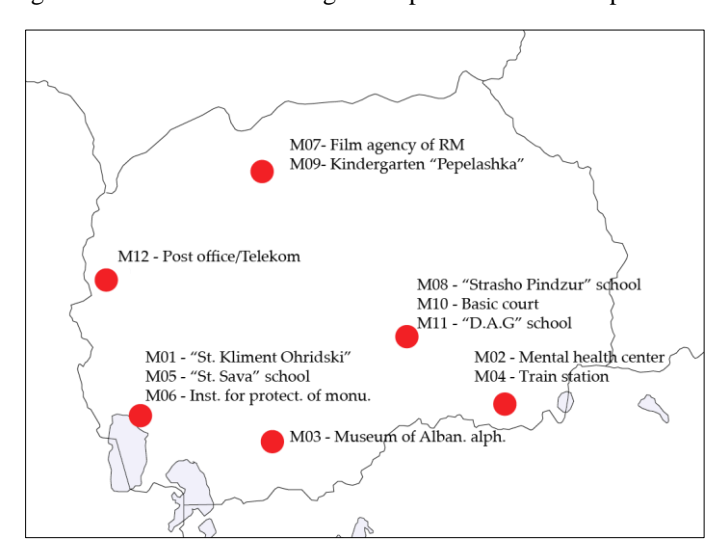


Figure 3. Geographical distribution of the buildings included in the study

Figure 4 presents the layout and photograph of a representative example (M11). The building is located in the Municipality of Kavadarci and was constructed in the early 20th century. It comprises a basement, ground floor, and two upper stories.

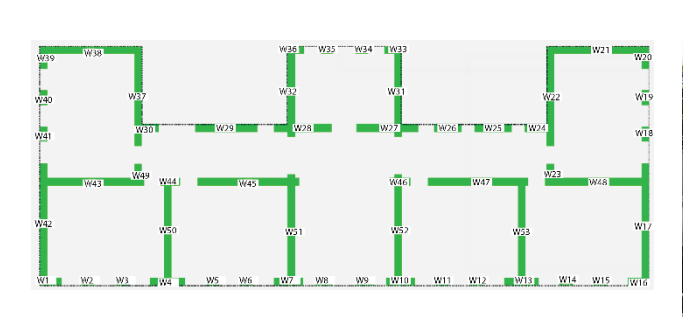




Figure 4. Layout (left) and photograph of the selected building (right)

The buildings selected for this study were primarily constructed using solid clay bricks and lime mortar, which is a commonly used material combination for unreinforced masonry structures in the Republic of North Macedonia prior to the 1963 earthquake. Based on field surveys and historical construction practices, it can be stated with a high degree of certainty that the vast majority of existing residential masonry buildings in the country are composed of this same material system. For the development of a reliable numerical model, accurate determination of the mechanical properties of the materials used is essential. However, unreinforced masonry is inherently a heterogeneous composite consisting of units (bricks) and mortar joints, which introduce significant variability in its mechanical response. This heterogeneity leads to a wide scatter in the experimentally determined properties, as observed in previous studies. Owing to numerous unknowns and inconsistencies in material quality and construction practices, direct laboratory testing of the constituent materials and assembled masonry elements is the most reliable method for obtaining physical and mechanical properties.

However, laboratory testing becomes particularly challenging when dealing with existing structures, as the procedures are destructive in nature and require the extraction of brick samples from the building. For this reason, permits for material sampling were obtained for only two buildings: The St. Sava School in Ohrid, which is one of the 12 selected buildings in this research, and a structure in Kichevo constructed during a similar historical period.

All the extracted bricks were solid clay units with approximate dimensions of $250 \text{ mm} \times 150 \text{ mm} \times 125 \text{ mm}$ (length × width × height). The brick density was calculated as the mass-to-volume ratio for each unit, resulting in a mean density of $1,722 \text{ kg/m}^3$. A comprehensive laboratory testing program was conducted, including compressive strength testing of individual bricks, compressive and flexural strength tests of mortar samples, and compressive strength testing of small masonry wall specimens (wallets). The preparation and testing of the bricks followed the Macedonian Standard MKS B.D 8.011 (B.D8.011., 07-4713/1). Tests were conducted using a hydraulically controlled testing system with gradual application of load until failure occurred. It is important to note that the mechanical properties of masonry are influenced not only by the type of brick and mortar but also by construction practices, age-related deterioration, and environmental exposure. As a result, significant variability in mechanical characteristics may be observed, even in experimental setups.

For the purpose of numerical simulation, Latin Hypercube Sampling (LHS) [70] was employed to generate representative material samples. Table 1 outlines the fixed material parameters, whereas Table 2 presents the mean values and standard deviations of the stochastic input variables, which reflect the material uncertainties.

Table 1. Material properties – fixed values

Characteristic	Value	Unit
Modulus of elasticity of masonry (E)	2450	MPa
Shear modulus of masonry (G)	490	MPa
Density of masonry (g)	1700	kg/m^3

Table 2. Material properties – Input parameters - Uncertainties

Characteristic	Mean Value	Unit	SD				
Material characteristics							
Compressive strength of masonry	2.45	MPa	2				
Initial shear strength of masonry	0.25	MPa	0.2				
Damping co	oefficients						
Bending failure	0.2	-	0.07				
Shear failure - bed joint sliding	0.9	-	0.3				
Shear failure - diagonal tension	0.44	-	0.15				
Loa	ıds						
Vertical load on slab (g+p)	4	kN/m²	2				
Vertical load on roof(g+p)	2	kN/m²	2				
Drifts							
Bending	0.39	[%]	0.2				
Shear	0.26	[%]	0.12				
Structure	Structure modeling						
Level of restrain	0.625	-	0.21				

Given the lack of local studies specific to unreinforced masonry in North Macedonia, the drift limits used in the current analysis were selected based on the database values for solid clay masonry [71], recommendations from Eurocode 8 – Part 3 (EC8-3, 2005), provisions in Italian seismic codes, and engineering judgment by the authors.

To account for the wall–floor interaction, a restraint factor α was introduced, allowing the numerical model to reflect the degree of restraint provided by slabs at the wall tops.

Structural safety verification was conducted using nonlinear static (pushover) analysis, in which the displacement demand caused by seismic loading was compared with the displacement capacity of the structure. The buildings were modeled using continuous shear wall elements over the height of the structure.

The verification methodology incorporates both the classic Capacity Spectrum Method (CSM) and N2 method [72]. The analysis included the generation of a nonlinear pushover curve derived by progressively increasing a predefined horizontal load distribution. All calculations were performed using the MINEA software [73].

The nonlinear capacity curves for individual walls are based on their shear and bending resistances, evaluated according to Eurocode provisions. For this, the drift and restraint levels are essential parameters. Once the drift limit is reached, the wall is assumed to lose its load-bearing capacity and its contribution is set to zero. In the modeling, the walls are idealized using Timoshenko beam elements, which capture both bending and shear deformations. Prior to yielding, the stiffness of the wall was computed as a superposition of the shear and bending stiffnesses in the equivalent beam formulation. The initial geometric and material properties, such as the moment of inertia and cross-sectional area, are determined as the first step in the modeling process.

2.3. Definition of Damage Grades

The third component of the methodology, illustrated in Figure 1, involves defining the damage indicator and associated damage grades. The damage limit states were determined based on the pushover curves calculated for each of the analyzed structures.

For unreinforced masonry buildings, deformation-based parameters are widely recognized as the most reliable indicators of structural damage. In line with this, the present study adopted displacement as the primary damage indicator. Two key displacement values were extracted from each pushover curve: Yield displacement (dy), marking the onset of inelastic behavior, and Ultimate displacement (du), representing the structural failure threshold.

To enable consistent classification of the damage, the pushover curve was divided into five intervals, each corresponding to a distinct damage grade. This segmentation provides a structured approach for interpreting the damage severity under increasing seismic demand and facilitates the mapping of displacement capacity to qualitative damage levels, ranging from no damage to near collapse.

The damage states are defined as follows [74, 75]:

DS0 – Initial Cracking: Defined as 70% of the displacement at DS1; indicates the appearance of the first visible crack. At this stage, the building behaved linearly, with only minor hairline cracks appearing.

- DS1 Slight Damage: Marks the transition from elastic to inelastic behavior on the capacity curve. The load–displacement curve shows the first reduction in stiffness as the individual walls start to enter the plastic range.
- DS2 Moderate Damage: Represents visible cracking; calculated as 0.5 (). The displacement reached the midpoint of the plateau region corresponding to the maximum shear capacity.
- DS3 Significant Damage: Occurs when the base shear decreases to 80% of the maximum value (0.8 Fb,max). One or more walls fail. DG3 is defined as 80% of the maximum shear force on the capacity curve, assuming that the building remains safe if the reduction from the maximum shear does not exceed 20%.
- DS4 Near Collapse: Defined as the displacement corresponding to a 50% reduction in the base shear capacity (0.5 · Fb,max). A critical number of walls are heavily damaged or fail, requiring a significant redistribution of the horizontal and vertical forces.

The third component of the methodology, illustrated in Figure 1, involves the definition of the damage indicator and the associated damage grades. Damage limit states are determined based on the pushover curves calculated for each of the analyzed structures.

3. Fragility and Reliability Curves

3.1. Design of Virtual Experiment and Statistical Processing

For each of the selected buildings, a virtual experiment was conducted to estimate the probability of exceeding specific damage states at various levels of seismic intensity. The first step involved generating an experimental dataset and defining the input samples using the Latin Hypercube Sampling (LHS) method. This process utilized predefined mean values, standard deviations, and boundary limits for all uncertain input parameters (input variables IV). In this manner, a virtual experiment was designed systematically. The seismic input was defined using the regionally specified response spectra. These spectra were scaled across a range from 0.01 g to 0.51 g in increments of 0.01 g, resulting in 51 distinct seismic intensity levels being applied in each analysis. Nonlinear static (pushover) analyses were performed, and performance-point displacements were computed for each input sample and for each seismic intensity level within the virtual experiment. Figure 5 illustrates the calculated performance point displacements for one representative building, subjected to seismic intensities ranging from 0.1 g to 0.4 g. Each point in the figure corresponds to a single realization from the virtual experiment. Additionally, a dataset containing drift values derived from pushover analysis for each realization was produced and stored.

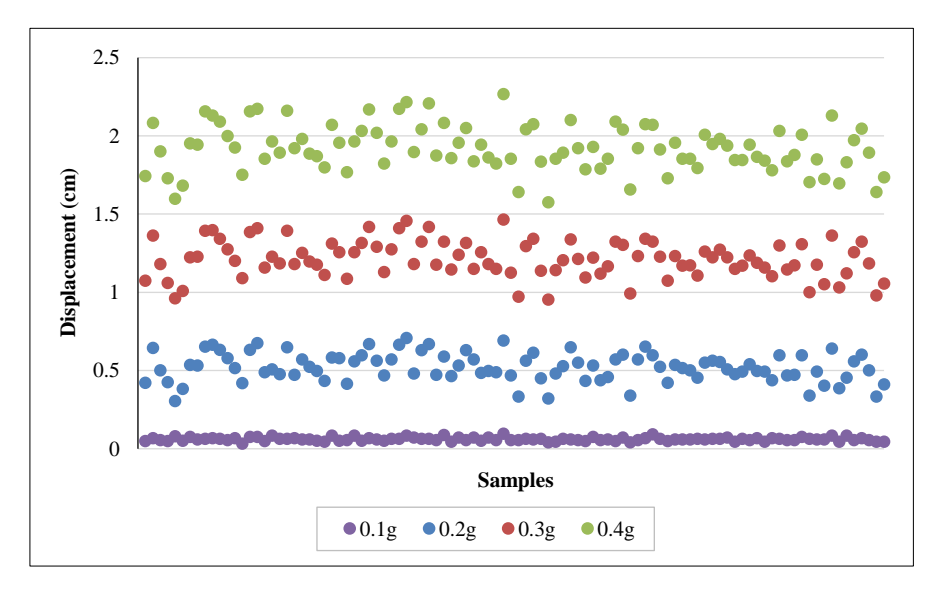


Figure 5. Results from virtual experiment

Each calculated performance point value was classified into an appropriate damage group based on the corresponding limit state values determined from the analysis. For each seismic intensity level, the total number of samples within each damage group was counted, resulting in the classification of all the samples into six damage groups. This classification is organized into a matrix that contains the distribution of damage states across all seismic levels. The probability of exceeding a particular damage state was then computed by dividing the number of samples that exceeded the specified

damage threshold by the total number of samples analyzed. The Maximum Likelihood Estimation method was applied to estimate the statistical parameters and generate fragility curves, the Maximum Likelihood Estimation (MLE) method is applied. The entire process of data analysis, statistical evaluation, and fragility curve generation was performed using custom-developed Python scripts. Figure 6 shows a schematic of the entire process.

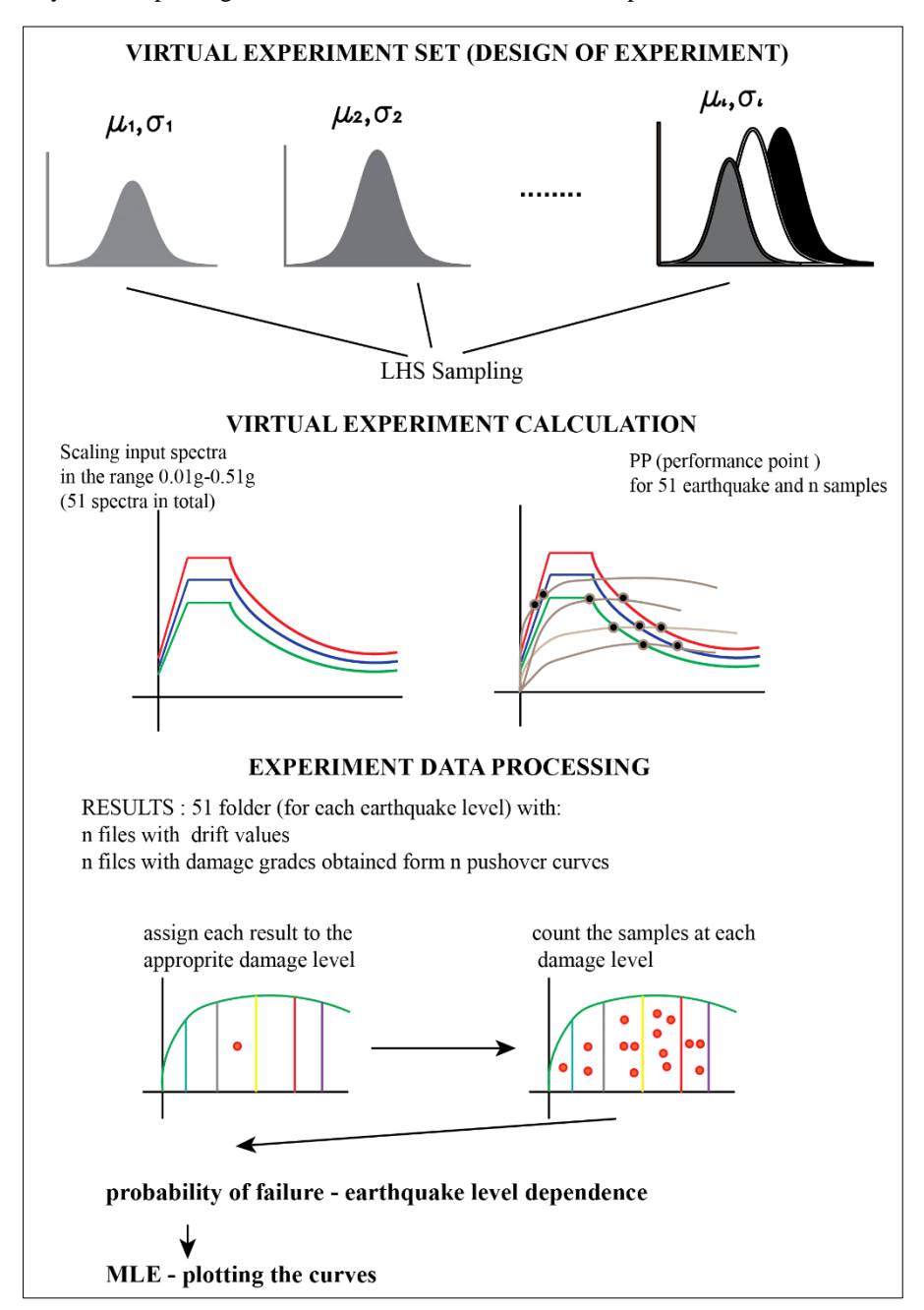


Figure 6. The procedure for obtaining the curves

The lognormal cumulative distribution function (CDF), presented in Equation 1, is the most commonly used representation of the seismic vulnerability function, describing the conditional probability of exceeding a specific threshold (limit state) for a given level of earthquake loading.

$$P(LS|Sa = x) = \phi\left(\frac{\ln x/\mu}{\beta}\right) \tag{1}$$

where, P(LS|Sa = x) represents the probability of exceeding a specific limit state given a ground motion of Sa = x, $\Phi()$ denotes the standard normal cumulative distribution function. The parameters μ and β correspond to the mean and standard deviation of $\ln Sa$.

Various approaches can be used to estimate μ and β including the method of moments, least squares, and maximum likelihood estimation. In this study, maximum likelihood estimation is employed to optimally fit the data derived from numerical simulations [76]. For computational purposes, the likelihood function is maximized as shown in Equation 2.

$$\left\{ \hat{\mu}, \hat{\beta} \right\} = \max_{\mu, \sigma} \sum_{i=1}^{m} \ln \binom{n_j}{z_j} + z_i \ln \varphi \left(\frac{\ln x_j / \mu}{\beta} \right) + (n_i - z_i) \ln \left(1 - \varphi \left(\frac{\ln x_i / \mu}{\beta} \right) \right) \tag{2}$$

Using the MLE approach and calculated damage probabilities, the values of median and logarithmic standard deviation are estimated for all of the limit state employed. Using these values and the logarithmic equation, the values of the exceeding probabilities are calculated. Also, the reliability index is computed and reliability functions are estimated for all of the damage states utilized.

Using all of the calculated values (displacements and damage grades) for all regions and all 12 buildings, the fragility and reliability curves for the following classes of unreinforced masonry structures are calculated (Figure 7):

- Fragility and reliability curves for the territory of Republic of North Macedonia
- Fragility curves for the 4 selected regions in the country.
- Fragility curves for regular and irregular in plan structures.

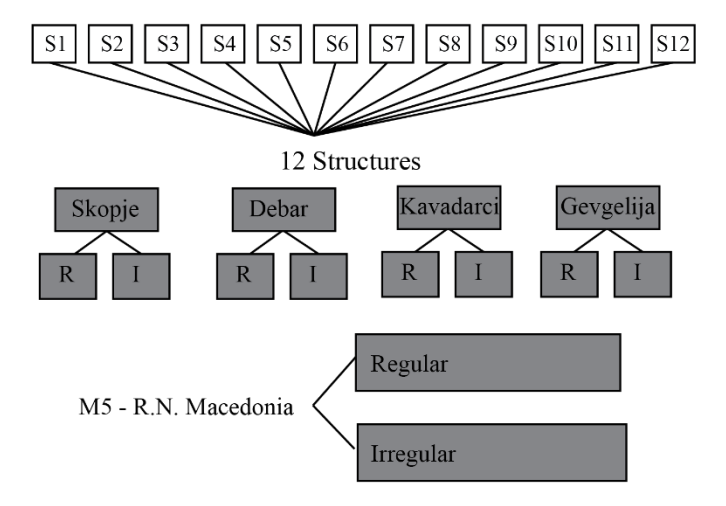


Figure 7. Classes of developed fragility curves

3.2. Fragility and Reliability Curves for the Territory of Republic of North Macedonia

Figure 8 presents the calculated fragility and reliability curves for the entire national territory, derived using comprehensive data on seismic input and structural typologies. These curves are based on the aggregation of information from various building types and seismic scenarios, ensuring a representative overview of the country's structural vulnerability.

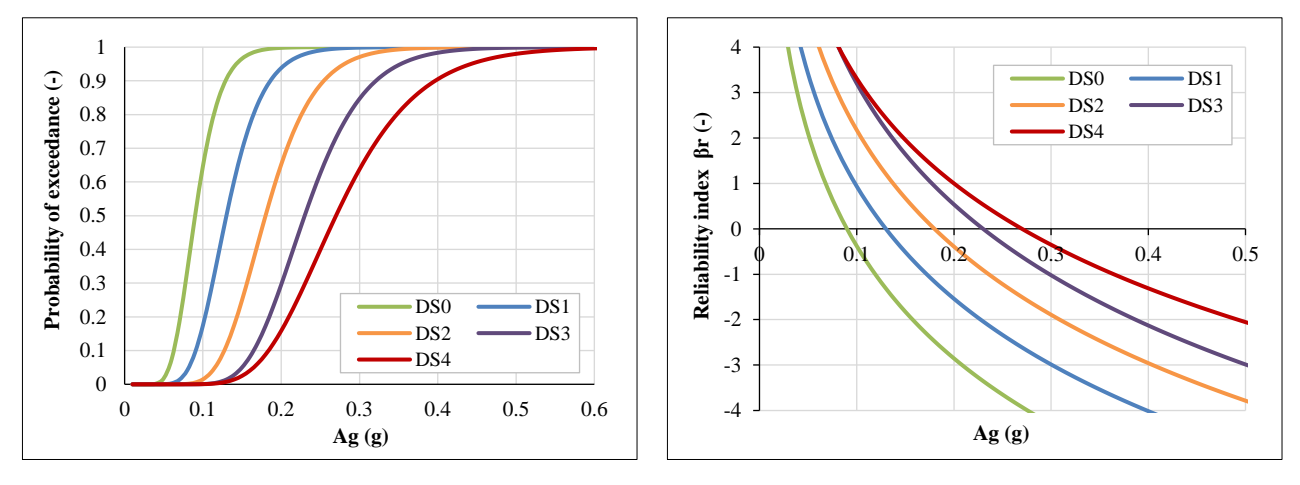


Figure 8. Fragility and reliability curves for the territory of Republic of North Macedonia

The estimated statistical parameters for all five damage states (DS0 through DS4), obtained through Maximum Likelihood Estimation (MLE), are summarized in Table 3. When assessing the probability of exceedance at a ground acceleration of 0.3g, which corresponds to the reference seismic intensity specified in the current national regulations for seismic design, the results show a 100% probability of exceedance for damage states DS0 to DS2.

For more severe damage states, DS3 and DS4, the probabilities are 85% and 64%, respectively. These results align well with observed damage patterns in masonry structures during past seismic events, thereby confirming the validity of the model.

Table 3. Estimated statistical parameters

	DS0	DS1	DS2	DS3	DS4
θ	0.09	0.13	0.18	0.23	0.27
β	0.28	0.28	0.27	0.26	0.30

At a lower seismic intensity of 0.1g, the curves indicate no exceedance for damage states DS2 through DS4. The probability of exceedance for DS1 is 20%, while DS0 stands at 60%. These values highlight the nonlinear increase in damage probability with rising seismic intensity, particularly for lower damage states.

The reliability curves, which are intrinsically linked to the probability of failure, provide further insight into structural performance under seismic loading. As the reliability index increases, the probability of failure decreases, enabling clear identification of structural safety zones. The zero crossing point on the reliability curve signifies a 50% probability of failure, effectively marking the threshold between safe and unsafe conditions. According to the generated curves, structures can be considered marginally safe at a seismic intensity of approximately 0.27g. Above this threshold, structural reliability increases, whereas below it, the probability of failure becomes unacceptably high.

The fragility and reliability curves developed for the entire territory offer a valuable tool for seismic risk assessment and serve as a baseline for comparing regional seismic responses. However, these curves should be complemented with region-specific assessments for more precise and effective earthquake preparedness and design strategies.

3.3. Region Sensitivity

Based on the previously described methodology, the fragility and reliability curves were calculated and plotted for the four selected regions. The proposed curves were derived by applying the estimated response spectra specific to each region to a consistent set of 12 representative buildings. The statistical analysis performed on the resulting data yielded estimated parameters, which are summarized in Tables 4 to 7, while the resulting fragility curves are illustrated in Figures 9 to 12.

Table 4. Estimated statistical parameters - Skopje

	DS0	DS1	DS2	DS3	DS4
θ	0.08	0.12	0.17	0.21	0.25
β	0.25	0.26	0.25	0.27	0.30

Table 5. Estimated statistical parameters - Debar

	DS0	DS1	DS2	DS3	DS4
θ	0.08	0.11	0.16	0.21	0.25
β	0.22	0.30	0.28	0.27	0.30

Table 6. Estimated statistical parameters - Gevgelija

	DS0	DS1	DS2	DS3	DS4
θ	0.10	0.13	0.18	0.23	0.27
β	0.22	0.27	0.29	0.29	0.30

Table 7. Estimated statistical parameters - Kavadarci

	DS0	DS1	DS2	DS3	DS4
θ	0.11	0.16	0.22	0.28	0.33
β	0.25	0.25	0.23	0.24	0.26

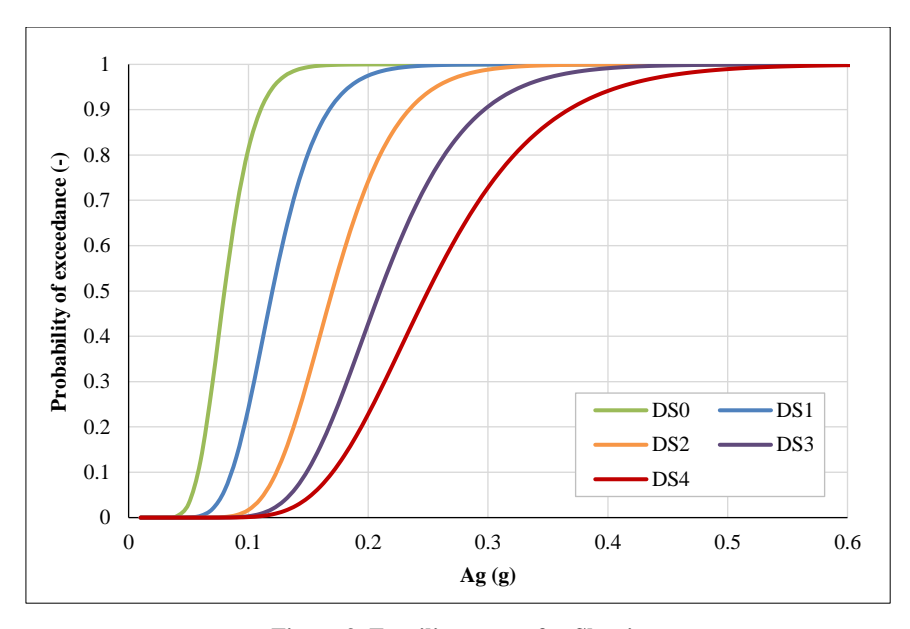


Figure 9. Fragility curves for Skopje

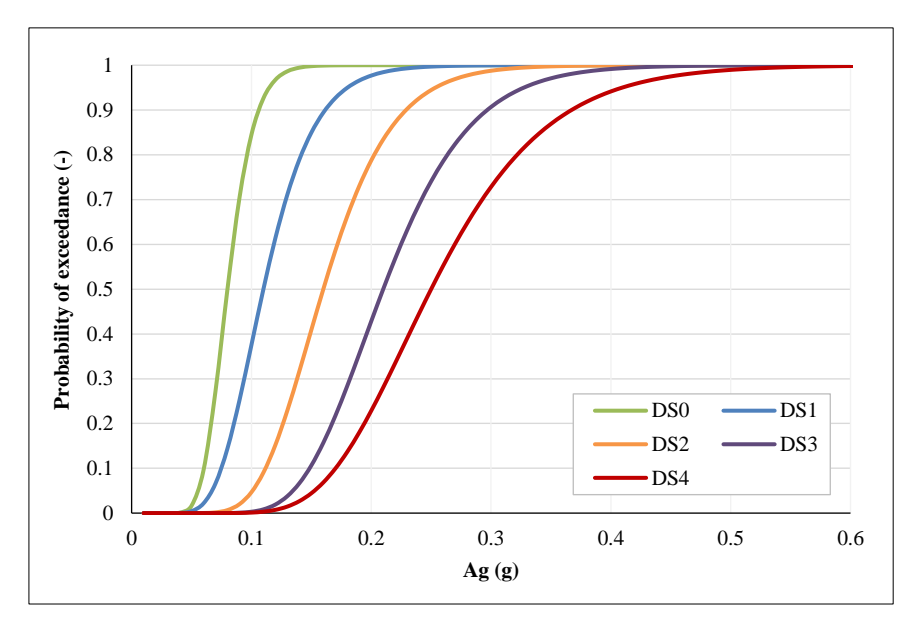


Figure 10. Fragility curves for Debar

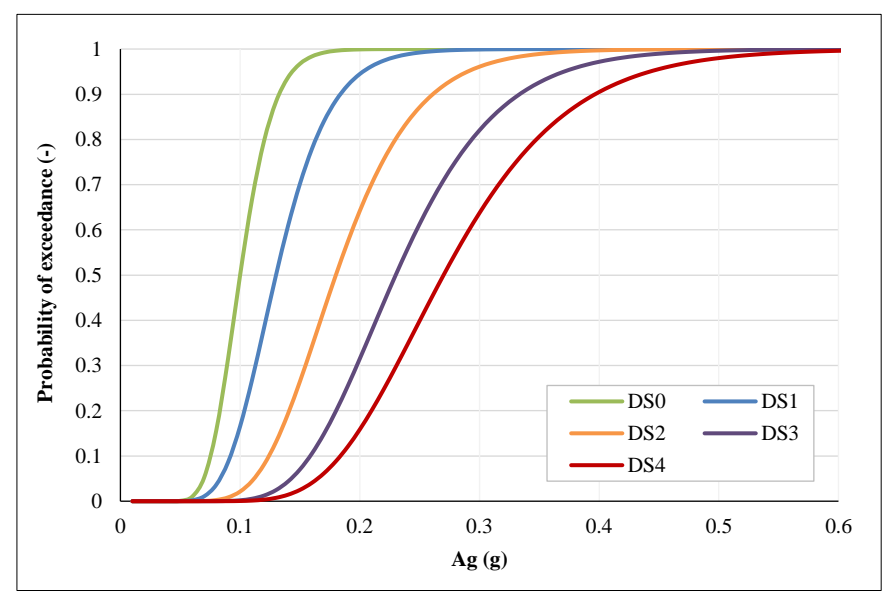


Figure 11. Fragility curves for Gevgelija

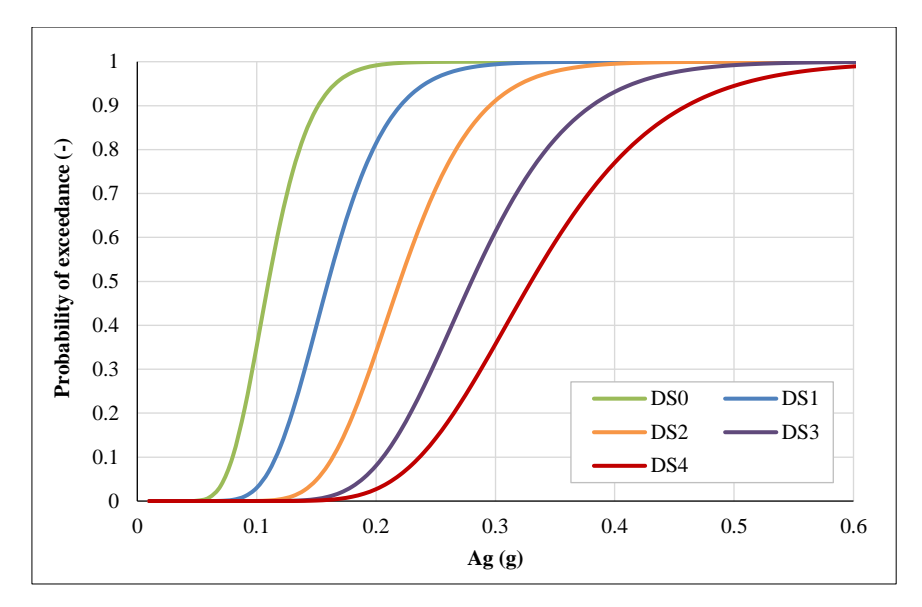


Figure 12. Fragility curves for Kavadarci

To evaluate the validity and practicality of using a single set of fragility curves for the entire country as opposed to region-specific curves, a comparative analysis was conducted. This analysis involved calculating the matrices of the relative errors for each region's curve with respect to the nationwide reference curve.

The results of this comparison indicate that for damage states DS0 through DS2, the relative differences between the regional and national curves are minimal, suggesting that a unified curve could reasonably represent these lower damage states across all four regions. However, for the more severe damage states, notable discrepancies were observed. Specifically, for damage state DS3, Skopje and Debar exhibited a relative error of +7.1%, whereas Kavadarci showed a significant underestimation of -27.6%. This implies that employing a single nationwide curve would lead to the underestimation of potential damage in Skopje and Debar and an overestimation in Kavadarci.

The divergence becomes even more pronounced for the damage state DS4. In this case, the relative error increased to +14.3% for Skopje and Debar and reached a substantial +44% for Kavadarci. These findings highlight the limitations of a uniform approach and underscore the importance of considering regional variations when assessing the seismic vulnerability and developing fragility curves.

In conclusion, although a single national fragility curve may provide a reasonable approximation for lower damage states, its application to higher damage states could lead to significant inaccuracies. Therefore, it is recommended that region-specific fragility curves be used, particularly when assessing higher levels of seismic damage, to ensure more accurate risk assessment, resource allocation, and mitigation planning.

3.4. Plan Sensitivity (Regular and Irregular)

All the selected structures were categorized into two primary groups based on their geometric configuration: regular and irregular, as previously defined. Fragility and reliability curves were developed separately for each group, and are presented in the following subsections to facilitate comparative analysis.

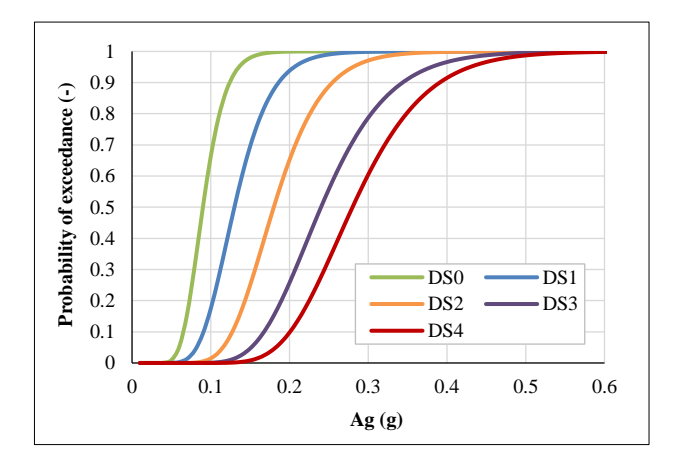
The estimated statistical parameters and corresponding damage matrices for unreinforced masonry (URM) structures classified as regular and irregular in plan were obtained using the nonlinear static analysis method outlined in earlier sections by applying the full set of response spectra to each group of structures. The resulting fragility curves are shown in Figure 13.

The comparison between the two groups revealed a consistently better seismic performance of regular structures relative to their irregular counterparts. This trend is evident across all damage states, indicating that plan irregularities have a notable influence on the vulnerability of URM buildings. The smoother distribution of seismic forces and more uniform deformation in regular structures likely contributed to their improved behavior under seismic loading.

To further quantify these differences, the relative error [%] was calculated by comparing the fragility curves of the irregular structures against those of the regular structures. At the intensity level of 0.3 g, the relative error is 3.7% for damage state DS3 and increases to 8% for damage state DS4. These discrepancies highlight the growing divergence in the expected performance between regular and irregular structures as damage severity increases.

In conclusion, the analysis clearly demonstrated that plan irregularity has a detrimental effect on the seismic performance of unreinforced masonry structures. Although differences may appear modest for moderate damage levels,

they become more pronounced at higher damage states. These findings underscore the importance of incorporating geometric regularity as a design criterion in seismic-prone regions, and suggest that irregular structures may require additional strengthening or design considerations to achieve comparable performance.



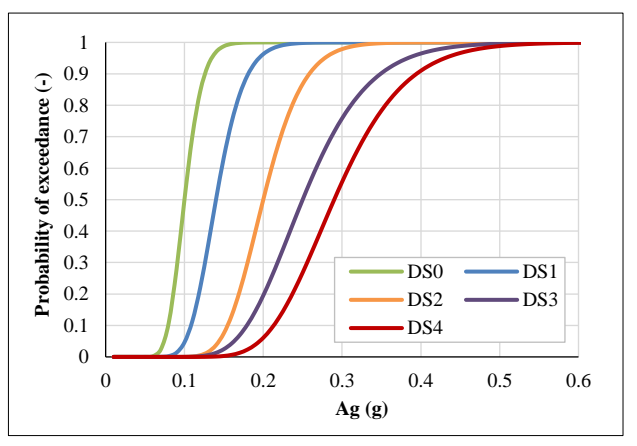


Figure 13. Fragility curves for regular and irregular structures

4. Conclusions

This study presents a comprehensive seismic vulnerability assessment of unreinforced masonry (URM) structures across various regions and structural typologies using fragility and reliability curves developed through nonlinear analysis and statistical modeling.

In the first part of the analysis, fragility and reliability curves were generated for four representative regions by applying region-specific seismic input data to a standardized set of 12 URM buildings. The results revealed that the use of a single national curve yielded acceptable approximations for the lower damage states (DS0–DS2). However, significant discrepancies were observed for higher damage states (DS3 and DS4). Specifically, Skopje and Debar showed a relative error of up to +14.3%, while Kavadarci showed an overestimation of 44% for DS4. These findings underscore the need for region-specific fragility curves to enhance the accuracy of damage prediction and risk assessment, particularly for severe seismic events.

In the second part, fragility and reliability curves are developed for the entire territory using the full dataset of seismic input and structural typologies. At the design-level intensity of 0.3 g, the probability of exceedance reached 100% for DS0–DS2, 85% for DS3, and 64% for DS4, values that align with the observed earthquake damage in similar structures. The reliability curves further indicated that the threshold for structural safety was approximately 0.27 g, below which the probability of failure exceeded 50%. This confirms that the seismic design reference level (0.3 g) is an appropriate benchmark for assessing the structural safety on a national scale.

The final part of the study focused on structural configuration by dividing the building set into regular and irregular structures in the plan. The fragility and reliability curves calculated for each subgroup revealed better seismic performance for regular structures across all damage states. A relative error analysis showed a difference of up to 8% at DS4 for irregular structures, confirming that plan irregularity increased vulnerability. This highlights the importance of promoting regularity in architectural design and considering additional reinforcements or design modifications for irregular URM buildings in seismic zones.

Beyond its analytical contributions, the proposed methodology for fragility curve development represents a novel and valuable approach that bridges region-specific building typologies and seismic inputs. This methodology provides a robust framework for long-term applications and policy development and offers several important benefits.

- The generated fragility curves for URM buildings, particularly the four region-specific sets, can be directly utilized by public authorities, such as the Crisis Management Center, to support seismic risk mapping and emergency preparedness across the country.
- If a comprehensive database of existing masonry structures in the Republic of North Macedonia is developed, categorizing buildings by structural system the fragility curves for regular and irregular configurations—can be applied in even more refined seismic risk assessments, enabling better-informed planning and targeted mitigation strategies.
- The fragility and reliability curves provide a visual and quantitative illustration of the expected damage following potential earthquake events, thereby enhancing public understanding and supporting scenario-based planning.

These results serve as a solid foundation for formulating a national risk-mitigation strategy, integrating scientific analysis with practical planning tools to improve disaster resilience at both regional and national levels.

5. Declarations

5.1. Author Contributions

Conceptualization, K.M. and E.D.J.; methodology, K.M.; software, K.M.; validation, E.D.J.; formal analysis, K.M.; investigation, K.M.; resources, E.D.J.; data curation, K.M.; writing—original draft preparation, K.M.; writing—review and editing, E.D.J.; visualization, K.M.; supervision, E.D.J.; project administration, K.M. All authors have read and agreed to the published version of the manuscript.

5.2. Data Availability Statement

The data presented in this study are available on request from the corresponding author.

5.3. Funding

The authors received no financial support for the research, authorship, and/or publication of this article.

5.4. Conflicts of Interest

The authors declare no conflict of interest.

6. References

- [1] Firoozi, A. A., & Firoozi, A. A. (2024). Geotechnical Innovations for Seismic-Resistant Urban Infrastructure. Journal of Civil Engineering and Urbanism, 14(3s), 346–355. doi:10.54203/jceu.2024.39.
- [2] Booth, E. (2018). Dealing with earthquakes: the practice of seismic engineering 'as if people mattered.' Bulletin of Earthquake Engineering, 16(4), 1661–1724. doi:10.1007/s10518-017-0302-8.
- [3] Freddi, F., Galasso, C., Cremen, G., Dall'Asta, A., Di Sarno, L., Giaralis, A., Gutiérrez-Urzúa, F., Málaga-Chuquitaype, C., Mitoulis, S. A., Petrone, C., Sextos, A., Sousa, L., Tarbali, K., Tubaldi, E., Wardman, J., & Woo, G. (2021). Innovations in earthquake risk reduction for resilience: Recent advances and challenges. International Journal of Disaster Risk Reduction, 60. doi:10.1016/j.ijdrr.2021.102267.
- [4] Davis, I., & Alexander, D. (2015). Recovery from Disaster, 303–308, Routledge, London, United Kingdom. doi:10.4324/9781315679808-20.
- [5] Salic Makreska, R., Drogreska, K., Sinadinovski, C., Neziri, Z., Jovanov, L., Milutinovic, Z., Pekevski, L., Najdovska, J., Atanasovska, D. C., & Tomic, D. (2023). Impact of Moderate Size Earthquakes through Skopje 2016 and Zagreb 2020 Case Studies. 2nd Croatian Conference on Earthquake Engineering 2CroCEE, 840–855. doi:10.5592/co/2crocee.2023.10.
- [6] Sinadinovski, C., & Cernih, D. (2019, January). Analysis of records from the M5. 2 September 2016 Skopje earthquake. Geophysical Research Abstracts (Vol. 21), EBSCO Industries, Birmingham, United States.
- [7] Romano, E., Negro, P., Formisano, A., Landolfo, R., Menna, C., Prota, A., & Hajek, P. (2023). Methodologies for the assessment of the combined seismic and energy retrofit of existing buildings: a new simplified method and application to case studies. Publications Office of the European Union, Luxembourg, Luxembourg.
- [8] Takewaki, I. (2015). Beyond Uncertainties in Earthquake Structural Engineering. Frontiers in Built Environment, 1. doi:10.3389/fbuil.2015.00001.
- [9] E. Rodriguez, M. (2024). Seismic-Resistant Design Regulations for Structures, Earthquake and Experimental Results Lessons. Journal of Building Technology, 6(2), 2545. doi:10.32629/jbt.v6i2.2545.
- [10] Hakim, R. A., Alama, M. S., & Ashour, S. A. (2014). Seismic Assessment of RC Building According to ATC 40, FEMA 356 and FEMA 440. Arabian Journal for Science and Engineering, 39(11), 7691–7699. doi:10.1007/s13369-014-1395-x.
- [11] Penelis, G., & Penelis, G. (2014). Seismic risk management. Concrete Buildings in Seismic Regions, CRC Press, Boca Raton, United States. doi:10.1201/b16399-19.
- [12] UNISDR, U. (2015, March). Sendai framework for disaster risk reduction 2015–2030. In Proceedings of the 3rd United Nations World Conference on DRR, Sendai, Japan (Vol. 1). Proceedings of the 3rd United Nations World Conference on DRR, 18 March, Sendai, Japan.
- [13] Bedini, M. A., & Bronzini, F. (2018). The post-earthquake experience in Italy. Difficulties and the possibility of planning the resurgence of the territories affected by earthquakes. Land Use Policy, 78, 303–315. doi:10.1016/j.landusepol.2018.07.003.
- [14] Mohammadi, S., De Angeli, S., Boni, G., Pirlone, F., & Cattari, S. (2024). Review article: Current approaches and critical issues in multi-risk recovery planning of urban areas exposed to natural hazards. Natural Hazards and Earth System Sciences, 24(1), 79–107. doi:10.5194/nhess-24-79-2024.

[15] Rajkumari, S., Thakkar, K., & Goyal, H. (2022). Fragility analysis of structures subjected to seismic excitation: A state-of-the-art review. Structures, 40, 303–316. doi:10.1016/j.istruc.2022.04.023.

- [16] Silva, V. (2019). Uncertainty and correlation in seismic vulnerability functions of building classes. Earthquake Spectra, 35(4), 1515–1539. doi:10.1193/013018EQS031M.
- [17] Shabani, A., Kioumarsi, M., & Zucconi, M. (2021). State of the art of simplified analytical methods for seismic vulnerability assessment of unreinforced masonry buildings. Engineering Structures, 239. doi:10.1016/j.engstruct.2021.112280.
- [18] Calvi, G. M., Pinho, R., Magenes, G., Bommer, J. J., Restrepo-Vélez, L. F., & Crowley, H. (2006). Development of seismic vulnerability assessment methodologies over the past 30 years. ISET Journal of Earthquake Technology, 43(3), 75–104. doi:10.63898/busy2147.
- [19] Kassem, M. M., Mohamed Nazri, F., & Noroozinejad Farsangi, E. (2020). The seismic vulnerability assessment methodologies: A state-of-the-art review. Ain Shams Engineering Journal, 11(4), 849–864. doi:10.1016/j.asej.2020.04.001.
- [20] Lagomarsino, S., Marino, S., & Cattari, S. (2019). Seismic Assessment of Existing URM Buildings in Codes: Comparison Between Different Linear and Nonlinear Static Procedures. Proceedings of the 7th International Conference on Computational Methods in Structural Dynamics and Earthquake Engineering (COMPDYN 2015), 3129-3136. doi:10.7712/120119.7137.19681.
- [21] Zentner, I., Gündel, M., & Bonfils, N. (2017). Fragility analysis methods: Review of existing approaches and application. Nuclear Engineering and Design, 323, 245–258. doi:10.1016/j.nucengdes.2016.12.021.
- [22] Ulrich, T., Negulescu, C., & Douglas, J. (2014). Fragility curves for risk-targeted seismic design maps. Bulletin of Earthquake Engineering, 12(4), 1479–1491. doi:10.1007/s10518-013-9572-y.
- [23] Camayang, J. P., Dela Cruz, O., & Grutas, R. (2024). Integrating Building- and Site-Specific and Generic Fragility Curves into Seismic Risk Assessment: A PRISMA-Based Analysis of Methodologies and Applications. CivilEng, 5(4), 1011–1041. doi:10.3390/civileng5040050.
- [24] Gusella, F., Bartoli, G., & Pintucchi, B. (2025). A simplified loss-based procedure for seismic risk mitigation at a territorial scale. Bulletin of Earthquake Engineering, 23(5), 1941–1968. doi:10.1007/s10518-025-02117-w.
- [25] Nocevski, N. K. (1993). Definition of empirical and theoretical models for assessment of vulnerability level in high rise buildings, PhD Thesis, Institute of Earthquake Engineering & Engineering Seismology (IZIIS), Skopje, Macedonia.
- [26] Petrovski, J., & Ristic, D. (1984). Reversed cyclic loading test of bridge column models. Report IZIIZ, 84-164.
- [27] Dumova-Jovanoska, E. (2000). Fragility curves for reinforced concrete structures in Skopje (Macedonia) region. Soil Dynamics and Earthquake Engineering, 19(6), 455-466. doi:10.1016/S0267-7261(00)00017-8.
- [28] Milutinovic, Z. V., & Trendafiloski, G. S. (2003). Risk-UE An advanced approach to earthquake risk scenarios with applications to different european towns. Contract: EVK4-CT-2000-00014, WP4: Vulnerability of current buildings, EVK4-CT-2000-00014, WP4: Vulnerability of Current Buildings; European Commission: Brussels, Belgium.
- [29] Ristic, J., Guri, Z., & Ristic, D. (2024). Optionally Reinforced Columns Under Simulated Seismic and Time Varying Axial Loads: Advanced HYLSER-2 Testing. Civil Engineering Journal, 10(10), 3253–3268. doi:10.28991/CEJ-2024-010-10-09.
- [30] Savor Novak, M., Atalic, J., Uros, M., Prevolnik, S., & Nastev, M. (2019). Seismic risk reduction in Croatia: mitigating the challenges and grasping the opportunities. Future Trends in Civil Engineering, 71–109. doi:10.5592/co/ftce.2019.04.
- [31] Moretić, A., Chieffo, N., Stepinac, M., & Lourenço, P. B. (2023). Vulnerability assessment of historical building aggregates in Zagreb: implementation of a macroseismic approach. Bulletin of Earthquake Engineering, 21(4), 2045–2065. doi:10.1007/s10518-022-01596-5.
- [32] Nikolić, Ž., Benvenuti, E., Runjić, L., Kozulić, V., & Škomrlj, N. O. (2022). Assessment of seismic vulnerability of existing masonry buildings in urban area. 10th International Congress of Croatian Society of Mechanics, 28-30 September, 2022, Pula, Croatia.
- [33] Marinković, M., Bošković, M., Đorđević, F., Krtinić, N., & Žugić, Ž. (2024). Seismic Risk Assessment in School Buildings: A Comparative Study of Two Assessment Methods. Buildings, 14(8), 2348. doi:10.3390/buildings14082348.
- [34] Predari, G., Stefanini, L., Marinković, M., Stepinac, M., & Brzev, S. (2023). Adriseismic Methodology for Expeditious Seismic Assessment of Unreinforced Masonry Buildings. Buildings, 13(2), 344. doi:10.3390/buildings13020344.
- [35] Churilov, S., & Dumova-Jovanoska, E. (2013). In-plane shear behaviour of unreinforced and jacketed brick masonry walls. Soil Dynamics and Earthquake Engineering, 50, 85–105. doi:10.1016/j.soildyn.2013.03.006.
- [36] Milkova, K., Šavor Novak, M., Marinkovic, M., & Dumova-Jovanoska, E. (2025). A Review of Existing Seismic Vulnerability Functions for Buildings in the Balkan Region. 3rd Croatian Conference on Earthquake Engineering 3CroCEE, 3, 1157–1168. doi:10.5592/co/3crocee.2025.53.

[37] Grünthal, G., & Lorenzo Martín, F. (2009). European Macroseismic Scale 1998, European Macroseismic Scale 1998: EMS-98. GFZ German Research Center for Geosciences, Potsdam, Germany.

- [38] Schneider, P. J., & Schauer, B. A. (2006). HAZUS—Its Development and Its Future. Natural Hazards Review, 7(2), 40–44. doi:10.1061/(asce)1527-6988(2006)7:2(40).
- [39] Mahrous, A., AbdelRahman, B., & Galal, K. (2024). Seismic collapse risk assessment and fragility analysis of reinforced masonry core walls with boundary elements using the FEMA P695 methodology. Journal of Building Engineering, 98, 111225. doi:10.1016/j.jobe.2024.111225.
- [40] Bulajic, B., & Manic, M. (2006). Selection of the appropriate methodology for the deterministic seismic hazard assessment on the territory of the Republic of Serbia. Facta Universitatis Series: Architecture and Civil Engineering, 4(1), 41–50. doi:10.2298/fuace0601041b.
- [41] Zanetti, L., Chiffi, D., & Petrini, L. (2023). Philosophical aspects of probabilistic seismic hazard analysis (PSHA): a critical review. Natural Hazards, 117(2), 1193–1212. doi:10.1007/s11069-023-05901-6.
- [42] Gerstenberger, M. C., Marzocchi, W., Allen, T., Pagani, M., Adams, J., Danciu, L., Field, E. H., Fujiwara, H., Luco, N., Ma, K. F., Meletti, C., & Petersen, M. D. (2020). Probabilistic Seismic Hazard Analysis at Regional and National Scales: State of the Art and Future Challenges. Reviews of Geophysics, 58(2), e2019RG000653. doi:10.1029/2019RG000653.
- [43] Cornell, C. A. (1968). Engineering seismic risk analysis. Bulletin of the Seismological Society of America, 58(5), 1583–1606. doi:10.1785/bssa0580051583.
- [44] McGuire, R. K. (2008). Probabilistic seismic hazard analysis: Early history. Earthquake Engineering & Structural Dynamics, 37(3), 329–338. doi:10.1002/eqe.765.
- [45] Milutinovic, Z., Salic, R., & Tomic, D. (2015). An overview on earthquake hazard and seismic risk management policies of Macedonia. Proceedings of the International Conference on Earthquake Engineering and Seismology (IZIIS-50), 12-16 May, 2015, Skopje, Northern Macedonia.
- [46] Das, T. K., Choudhury, S., & Das, P. (2024). Correlation between seismic performance levels and damage index for regular RC frame buildings designed using the unified performance-based design method. Journal of Building Engineering, 96, 110565. doi:10.1016/j.jobe.2024.110565.
- [47] McGuire, R. K. (2001). Deterministic vs. probabilistic earthquake hazards and risks. Soil Dynamics and Earthquake Engineering, 21(5), 377–384. doi:10.1016/S0267-7261(01)00019-7.
- [48] Wang, Z. (2011). Seismic hazard assessment: Issues and alternatives. Pure and Applied Geophysics, 168(1–2), 11–25. doi:10.1007/s00024-010-0148-3.
- [49] Sen, T. K. (2009). Probabilistic Seismic Hazard Analysis. In Fundamentals of Seismic Loading on Structures. John Wiley & Sons, Hoboken, United States. doi:10.1002/9780470742341.ch7.
- [50] Huang, D., Wang, J. P., Brant, L., & Chang, S. C. (2012). Deterministic Seismic Hazard Analysis Considering Non-controlling Seismic Sources and Time Factors. Scalable Uncertainty Management. SUM 2012. Lecture Notes in Computer Science, 7520, Springer, Berlin, Germany. doi:10.1007/978-3-642-33362-0_42.
- [51] Herrero-Barbero, P., Álvarez-Gómez, J. A., Tsige, M., & Martínez-Díaz, J. J. (2023). Deterministic seismic hazard analysis from physics-based earthquake simulations in the Eastern Betics (SE Iberia). Engineering Geology, 327. doi:10.1016/j.enggeo.2023.107364.
- [52] Gupta, I. D. (2002). the State of the Art in Seismic Hazard Analysis. ISET Journal of Earthquake Technology, 311. doi:10.63898/wnkz4526.
- [53] Elnashai, A. S.-E., & El-Khoury, R. R. (2004). Deterministic Assessment of Seismic Hazard. Earthquake Hazard in Lebanon. World Scientific Publishing, Singapore. doi:10.1142/9781848161177_0010.
- [54] Ansari, A., Rao, K. S., & Jain, A. K. (2021). Seismic Hazard and Risk Assessment in Maharashtra: A Critical Review. Seismic Hazards and Risk. Lecture Notes in Civil Engineering, 116, Springer, Singapore. doi:10.1007/978-981-15-9976-7_4.
- [55] Magrin, A., Peresan, A., Kronrod, T., Vaccari, F., & Panza, G. F. (2017). Neo-deterministic seismic hazard assessment and earthquake occurrence rate. Engineering Geology, 229, 95–109. doi:10.1016/j.enggeo.2017.09.004.
- [56] Panza, G. F., Romanelli, F., & Vaccari, F. (2001). Seismic wave propagation in laterally heterogeneous anelastic media: Theory and applications to seismic zonation. Advances in Geophysics Volume 43, 1–95, Elsevier, Amsterdam, Netherlands. doi:10.1016/s0065-2687(01)80002-9.
- [57] Sarwar, F., Vaccari, F., & Magrin, A. (2022). Neo-deterministic seismic hazard assessment for Pakistan. Earthquakes and Sustainable Infrastructure, 543–558, Elsevier, Amsterdam, Netherlands. doi:10.1016/b978-0-12-823503-4.00014-2.

[58] Arsovski, M. (1960). Some characteristics of the tectonic features of the central part of Pelagonian horst anticlinorium and its relation to the Vardar Zone. Geologic Survey of SRM, Skopje, 7, 76-94.

- [59] Cavazza, W., Roure, F., Spakman, W., Stampfli, G. M., & Ziegler, P. A. (2004). The TRANSMED Atlas. The Mediterranean Region from Crust to Mantle. Springer, Berlin, Germany. doi:10.1007/978-3-642-18919-7.
- [60] Milkova, K., Dumova-Jovanovska, E., Drogreshka, K., Chernih-Anastasovska, D., Pekevski, L., Romanelli, F., ... & Panza, G. (2018). Region specific application of neo-deterministic analysis for reliable seismic hazard assessment. 16th European Conference on Earthquake Engineering, 18-21 June, 2018, Thessaloniki, Greece.
- [61] Milkova, K., Dumova-Jovanoska, E., Vaccari, F., Romanelli, F., & PANZA, G. F. (2019). Application of Neodeterministic Analysis for North Macedonia. Scientific Journal of Civil Engineering, 8(2), 91–94. doi:10.55302/sjce1982091m.
- [62] Press, F., & Brace, W. F. (1966). Earthquake prediction. Science, 152(3729), 1575–1584. doi:10.1126/science.152.3729.1575.
- [63] Dumova-Jovanoska, E., & Milkova, K. (2022). NDSHA-based vulnerability evaluation of precode buildings in Republic of North Macedonia: novel experiences. Earthquakes and Sustainable Infrastructure, Elsevier, Amsterdam, Netherlands. doi:10.1016/b978-0-12-823503-4.00023-3.
- [64] Panza, G. F. (2017). NDSHA: robust and reliable seismic hazard assessment. arXiv Preprint, arXiv:1709.02945. doi:10.48550/arXiv.1709.02945.
- [65] Fasan, M., Amadio, C., Noè, S., Panza, G., Magrin, A., Romanelli, F., & Vaccari, F. (2015). A new design strategy based on a deterministic definition of the seismic input to overcome the limits of design procedures based on probabilistic approaches. arXiv Preprint, arXiv:1509.09119. doi:10.48550/arXiv.1509.09119.
- [66] Panza, G. F., Vaccari, F., Romanelli, F., Amadio, C., Fasan, M., & Magrin, A. (2016). A seismological and engineering perspective on the 2016 Central Italy earthquakes. International Journal of Earthquake and Impact Engineering, 1(4), 395. doi:10.1504/ijeie.2016.10004076.
- [67] Dumova-Jovanoska, E., Aleksovski, G., Denkovska, L., Churilov, S., Milkova, K., Bogoevska, S., & Micevski, S. (2020). Seismic Vulnerability of Existing Masonry Buildings-Project Seismowall, Recent Results. 17th World Conference on Earthquake Engineering, 13-18 September, 2020, Sendai, Japan.
- [68] Dumova-Jovanoska, E., Aleksovski, G., Denkovska, L., Churilov, S., Milkova, K., Bogoevska, S., & Micevski, S. (2021). Seismic Vulnerability of Existing Masonry Buildings in the Balcan Area Case North Macedonia. 1st Croatian Conference on Earthquake Engineering, 129–140. doi:10.5592/co/1crocee.2021.159.
- [69] Churilov, S., Micevski, S., & Dumova-Jovanoska, E. (2018). Ambient vibration testing of public unreinforced masonry buildings from the beginning of the 20th century. Proceedings of the 16th European Conference on Earthquake Engineering, 18-21 June, 2018, Thessaloniki, Greece.
- [70] van der Mensbrugghe, D. (2023). A Summary Guide to the Latin Hypercube Sampling (LHS) Utility. GTAP Working Paper, 94. doi:10.21642/gtap.wp94.
- [71] Morandi, P., Albanesi, L., Graziotti, F., Li Piani, T., Penna, A., & Magenes, G. (2018). Development of a dataset on the in-plane experimental response of URM piers with bricks and blocks. Construction and Building Materials, 190, 593–611. doi:10.1016/j.conbuildmat.2018.09.070.
- [72] Fajfar, P., & Gašperšič, P. (1996). The N2 method for the seismic damage analysis of RC buildings. Earthquake Engineering and Structural Dynamics, 25(1), 31–46. doi:10.1002/(SICI)1096-9845(199601)25:1<31::AID-EQE534>3.0.CO;2-V.
- [73] SDA-solutions GmbH (2025). Design and analysis of masonry buildings, SDA-solutions GmbH, Herzogenrath, Germany.
- [74] Kappos, A. J., & Papanikolaou, V. K. (2016). Nonlinear Dynamic Analysis of Masonry Buildings and Definition of Seismic Damage States. The Open Construction and Building Technology Journal, 10(1), 192–209. doi:10.2174/1874836801610010192.
- [75] Rosin, J., Butenweg, C., Boesen, N., & Gellert, C. (2018). Evaluation of the Seismic Behavior of a Modern URM-Building during the 2012 Northern Italy Earthquakes. Proceedings of the 16th European Conference on Earthquake Engineering, 18-21 June, 2018, Thessaloniki, Greece.
- [76] Baker, J. W. (2015). Efficient analytical fragility function fitting using dynamic structural analysis. Earthquake Spectra, 31(1), 579–599. doi:10.1193/021113EQS025M.